Decoherence-induced strongly sub-Poissonian nonlocality

Qing Xu
School of Electronic Engineering, Huainan Normal University, Huainan 232038, People's Republic of China

(Received 16 June 2023; revised 5 July 2023; accepted 20 September 2023; published 3 October 2023)

Quantum decoherence tends to bring about the emergence of the classical from the quantum world through the interaction of a quantum system with the environment, which is the main impediment to the realization of quantum information processing. Counterintuitively, we propose that the decoherence enables the creation of a bright source of strongly sub-Poissonian nonlocality. The absence of the decoherence makes such a source impossible. Decoherence is devised to be adjustable and manipulable on the basis of the dressed-atom approach and combination mode technique. The strong sub-Poissonianity and robust Bell violation are originated from the large squeezing parameter of the reservoir pertaining to the controllable decoherence within the framework of the reservoir theory.

DOI: 10.1103/PhysRevA.108.043701

I. INTRODUCTION

Einstein, Podolsky, and Rosen (EPR) illustrated the inconsistency between the complete description of reality of the local realism and the completeness of quantum mechanics [1]. This spurred the exploration of the quantum nonlocality as one of the most profound features of quantum mechanics. In response to a quantitative test on quantum nonlocality of a composite system, Bell proposed an important inequality imposed by the local hidden variable theory [2,3]. Apart from being of fundamental significance [4–13], the Bell quantum violation plays a crucial role in the security of quantum communication protocols against individual attacks in quantum information processing [14,15].

The dynamical evolution of nonclassical correlation should be unitary in the ideal condition, thus quantum decoherence would not take place. Nevertheless, the system of interest can never be rigorously isolated from its surrounding environment with a large number of degrees of freedom. As a consequence, their interaction yields the decoherence of the system. Naturally, two realistic and critical questions arise. Is the nonlocal or nonclassical correlation sufficiently robust against the decoherence? The answer to the question as to what extent the nonlocal or nonclassical correlations like Bell nonlocality and entanglement should hold when going towards "classical" systems is as yet unknown. On the one hand, the concept of decoherence plays a pivotal role in understanding the appearance of noise in quantum systems and exploring the boundary between the classical regime and quantum realm. More often than not, the decoherence results in the substantial degradation or even complete inhibition of the nonlocal correlation of a target composite system [16–18]. The loss of quantum properties or the irreversible loss of information on the system can be interpreted as a result of the dynamical interaction between the system of concern and its surrounding environmental degrees of freedom. On the other hand, the decoherence has aroused great interest in quantum technologies based on the principles of quantum mechanics including quantum entanglement and quantum superposition. Compared to the more realistic physical systems, the idealized and isolated counterparts in the standard textbook of quantum mechanics are inadequate to find widespread applications in quantum information and nanotechnology, which require a detailed analysis of the limits due to the system-reservoir coupling. The decoherence corresponds to a tendency for the qubits to be extremely fragile and unable to stay in a superposition of quantum states or entangled states in the realistic situation. As a consequence, the decoherence becomes one of the biggest obstacles in quantum computing, and is, in particular, regarded as the quantum computer's greatest impediment owing to the irreversible loss of information. Therefore, it is of paramount importance to modify and manipulate quantum decoherence in an attempt to attain the desired spontaneous emission and even strong nonclassical correlation. A typical method is by tailoring the electromagnetic environment. Examples are the enhanced spontaneous emission [19], inhibited spontaneous emission [20], suppression, and enhancement of resonance fluorescence [21]. Another well-known way is by application of the artificial atomic or cavity reservoir [22,23].

In this paper, we have recourse to the dressed-atom approach and the combination mode technique for the purpose of not only controlling and manipulating the decoherence but also gaining a better insight into the physical mechanism, and obtain a bright source of strongly sub-Poissonian nonlocality by the dissipation mechanism at steady state. First, the decoherence usually gives rise to the quantum-to-classical transition. However, nothing in the principles of quantum mechanics hinders the composite system from attaining stationary strong nonlocality by quantum decoherence [22,23]. Second, the decoherence is engineered to yield the stationary pure two-mode squeezed vacuum state for the combination modes, and thus ultimately pulls the combination modes into the desired sub-Poissonian nonlocal regime with ultralarge photon occupation number. The arbitrarily large squeezing parameters are experimentally feasible in the atomic systems. The robust nonlocality enables the protection of quantum communication protocols from being eavesdropped on by the third party [14,15]. Third, the sub-Poissonian state of light

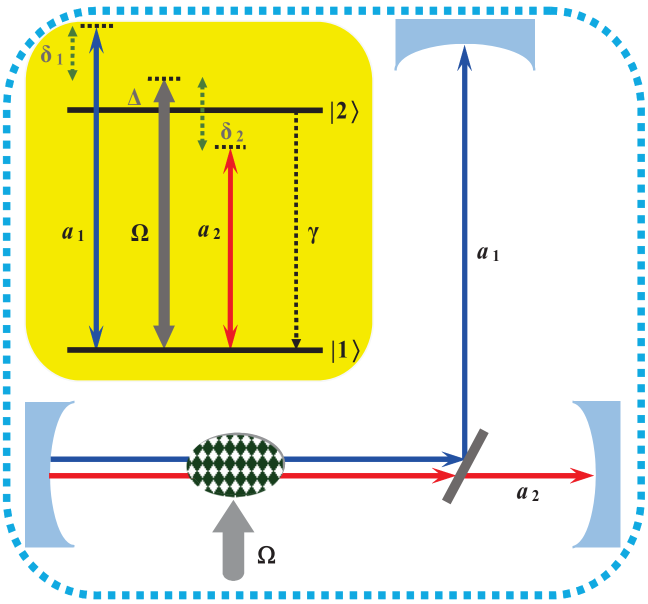

FIG. 1. The two-level atomic medium enclosed inside a doubly resonant cavity. The atom is coupled with Rabi frequency Ω to a coherent external field propagating transverse to the cavity axis and treated classically. Two cavity modes a_1 and a_2 are built up along the cavity axis and treated quantum mechanically.

[16–18,24–27] serves as a direct measure of the particle aspect of light in line with the field quantization, while both the Poissonian and the super-Poissonian regimes reveal the wave aspect of light.

The current scheme is based on the four-wave mixing and associated with the dissipation from the two original cavity modes by coupling to the two independent reservoirs, respectively, in the ordinary vacuum states and the dissipation from the atom via spontaneous emission into the background modes other than the privileged cavity modes. The central focus is on the recombination of the two cavity photon modes and on the investigation of the possibilities to obtain nonclassical states in the sub-Poissonian regime at a steady state and to study the robustness of nonclassical states. It is the four-wave mixing in combination with the suitable choice of the combination modes that necessarily brings about the two-mode-squeezed vacuum reservoir. The pair of combination modes is prepared in the stationary nonclassical state by the dissipation, independently of the initial state of the cavity modes.

II. MASTER EQUATION IN THE DRESSED-ATOM PICTURE

We consider a doubly resonant cavity enclosing a two-level atom with a ground state $|1\rangle$ and an excited state $|2\rangle$ (see the inset in Fig. 1). The two (original) cavity modes $a_{1,2}$ are coupled with strengths $g_{1,2}$ to the atom, which is, in turn, driven by a coherent external field with Rabi frequency Ω. The present scheme illustrates a good prospect of the application of the four-wave mixing. The application of the external field to a single two-level atom saturates the atomic transition and causes the separation of the states within an atomic level and thus the formation of the dressed states [28], which constitute a ladder of doublets with interdoublet separated by the external field frequency and intradoublet spaced by the generalized (detuned) Rabi frequency of the strong driving field. In the dressed-atom basis the singly dressed atomic system becomes a multilevel atom with three different transition frequencies and four nonvanishing dipole moments between the neighboring manifolds. The atom-cavity coupling allows for the intrinsically deterministic photon emission. As a consequence, the emission into the (original) cavity modes is enhanced by the resonant coupling with the Rabi sidebands. This is the underlying physical mechanism referred to as four-wave mixing [29–37] in our scheme, where the two photons of the pump modes are transformed into a pair of photons of two distinct signal modes simultaneously, ensuring no violation of the conservation of energy. The four-wave mixing process cannot occur in the scheme involving the interaction of the atom with a single cavity mode [38–41]. The four-wave mixing is one of the basic processes and opens an avenue for the generation of nonclassical light [30,31,34–37].

To be noted, here we invoke not the usual bare-state representation but the dressed-atom picture [28], which provides useful insight into the dynamics of this system and the physical mechanism. Contrary to the master equation in the bare-state representation shown in Appendix A, the counterpart in the dressed-state picture is written in terms of the combination modes as (for more details, see Appendixes B and C)

$$\dot{\varrho} = -\frac{i}{\hbar}[\mathcal{H}, \varrho] + \mathcal{L}_{\rm at}\varrho + \mathcal{L}_{\rm cav}\varrho, \tag{1}$$

where $\mathcal{H}$ is written in the form

$$\mathcal{H} = \begin{cases} \hbar\mathcal{G}A_1\sigma_{+-} + \text{H.c.}, & \text{if } \Delta > 0, \\ \hbar\mathcal{G}A_2^\dagger\sigma_{+-} + \text{H.c.}, & \text{if } \Delta < 0. \end{cases} \tag{2}$$

Here the combination modes A_l are connected to the original individual operators a_l through the squeezing transformation $A_l = \mathcal{S}a_l\mathcal{S}^\dagger$ $(l = 1, 2)$, where the squeeze operator reads as $\mathcal{S} = \exp(ra_1a_2 - ra_1^\dagger a_2^\dagger)$ [16–18], with $\tanh r = \tan^2\beta$ and $\beta = \frac{1}{2}\arctan\frac{|\Omega|}{|\Delta|}$, $\Delta = \omega_{21} - \omega_{\rm L}$ being the detuning of the atomic resonance transition frequency ω_{21} from the driving field frequency $\omega_{\rm L}$. The coupling strength $\mathcal{G}$ is written as $\mathcal{G} = \mathfrak{g}\sqrt{\cos(2\beta)}$, where we assume that $|g_1| = |g_2| = \mathfrak{g}$ for simplicity. $\sigma_{\mathfrak{s}\mathfrak{s}'} = |\mathfrak{s}\rangle\langle\mathfrak{s}'|$ are the atomic operators, $(\mathfrak{s}, \mathfrak{s}' = \pm)$, where $|\pm\rangle$ are the dressed states [28]

$$\begin{aligned} |+\rangle &= \sin\theta|1\rangle + \cos\theta|2\rangle, \\ |-\rangle &= \cos\theta|1\rangle - \sin\theta|2\rangle, \end{aligned} \tag{3}$$

with $\tan(2\theta) = |\Omega|/\Delta$ and $|\Omega| \gg (\gamma, \kappa_l, |g_l\langle a_l\rangle|)$, $(l = 1, 2)$.

With reference to Eq. (2), the introduction of combination modes results in the detuning-dependent coherent interaction of the atom with the quantized radiation fields. The construction of combination modes finds wide application in the quantum beat laser, multimode squeezed states, and multipartite entanglement [42–47]. On the space spanned by the combination modes, the resulting coherent interaction shows dependence on the sign of the atom–driving-field detuning, in analogy with a piecewise function in classical physics. Moreover, the strength of the coherent interaction is dependent on the ratio of the external driving field Rabi frequency (at resonance) to the atom-driving-field detuning. Apparently, this differs from the standard Jaynes-Cummings models extensively discussed in, e.g., Refs. [38–41]. As shown in the preceding scenario, the interaction of the dressed atom with one (the other) combination mode is described by the Jaynes-Cummings (anti-Jaynes-Cummings) Hamiltonian for the positive (negative) values of the detuning. This has roots in the underlying four-wave mixing mentioned above.

The damping term $\mathcal{L}_{\rm at}\varrho$ in Eq. (1) is recast into the form

$$\mathcal{L}_{\rm at}\varrho = \sum_{j=1}^{3}\Gamma_j \mathcal{D}[O_j]\varrho, \tag{4}$$

where the superoperator $\mathcal{D}[O]\varrho$ is defined as $\mathcal{D}[O]\varrho = O\varrho O^\dagger - \frac{1}{2}(O^\dagger O\varrho + \varrho O^\dagger O)$. The operators O_j in Eq. (4) are explicitly given by $O_1 = \sigma_{-+}$, $O_2 = \sigma_{+-}$, and $O_3 = \sigma_{++} - \sigma_{--}$, with $\Gamma_1 = \gamma\cos^4\theta$, $\Gamma_2 = \gamma\sin^4\theta$, and $\Gamma_3 = \gamma\cos^2\theta\sin^2\theta$. The term $\mathcal{D}[O_1]\varrho$ indicates the spontaneous emission from the dressed state $|+\rangle$ within the upper manifold to the dressed state $|-\rangle$ within the lower manifold, $\mathcal{D}[O_2]\varrho$ reveals the incoherent excitation from $|-\rangle$ within the lower manifold to $|+\rangle$ within the upper manifold, and $\mathcal{D}[O_3]\varrho$ represents the decay of the atomic polarization [48].

The damping term $\mathcal{L}_{\rm cav}\varrho$ is rewritten as

$$\begin{aligned}\mathcal{L}_{\rm cav}\varrho = &\kappa(N+1)\sum_{l=1,2}\mathcal{D}[A_l]\varrho + \kappa N\sum_{l=1,2}\mathcal{D}[A_l^\dagger]\varrho \\ &- \kappa M\sum_{\substack{k\neq l;\\ k,l=1,2}}(\mathcal{D}[A_k, A_l]\varrho + \text{H.c.}),\end{aligned} \tag{5}$$

where $\mathcal{D}[O_1, O_2]\varrho = O_1\varrho O_2 - \frac{1}{2}(O_2O_1\varrho + \varrho O_2O_1)$, we assume that $\kappa_1 = \kappa_2 = \kappa$. The parameters N and M account for the effect of the external environment on the modes $A_{1,2}$. The effective mean photon number per mode of the engineered reservoir N takes the form $N = \sinh^2 r$ and the intermode correlation function M also signifies the "squeezing" of the reservoir and is given by $M = \frac{1}{2}\sinh(2r)$. Furthermore, the squeezing effect of the current reservoir is enhanced with the decrease in the coupling strength $\mathcal{G}$ in Eq. (2).

As indicated from Eq. (5), the introduction of combination modes opens up interesting possibilities for the emergence of the intrinsic two-mode-squeezed vacuum reservoir. With the suitable choice of the combination modes, the four-wave mixing yields the two-mode-squeezed vacuum reservoir in a natural fashion. The reservoir is present on the space spanned by the pair of the combination modes, but absent on that spanned by the two (original) individual modes. There are, in principle, two key quantities characterizing the squeezed vacua. One is the mean photon number of the bath vacua, and the other is the magnitude or strength of the two-photon correlations associated with the phase-sensitive properties. Both quantities account for the frequency dependence of the vacuum modal density for the specified surrounding environment [16–18,38–41], and rest with the intrinsic property of the environment itself. More often than not, the functional dependence on the frequency is suppressed for simplicity. However, for the present scheme, the resultant squeezing parameter is determined by the external driving field Rabi frequency (at resonance) and the atom–driving-field detuning. More importantly, the controllable squeezing parameter varies continuously from negligibly small to infinitely large values. This is also applicable to the mean photon number of the squeezed vacuum and the magnitude of the two-photon correlations.

It follows from the master equation (1) that in the limit of $|\Delta| \to 0$ the combination modes $A_{1,2}$ are prepared asymptotically into the stationary two-mode squeezed vacuum state

$$|\psi\rangle_{\rm ss} = \mathcal{S}^\dagger(|0\rangle_1 \otimes |0\rangle_2), \tag{6}$$

which is generated at the rate of κ by the dissipation.

III. LANGEVIN EQUATIONS

In the following, attention is turned to addressing the time evolution of the field operators for simplicity. Our focus is first concentrated on the case of $\Delta > 0$. Having available the master equation (1) and the cyclic properties of the trace [17], the Langevin equations for $A_{1,2}$ are derived as

$$\begin{aligned}\dot{A}_1 &= -\frac{\kappa}{2}A_1 - i\mathcal{G}\sigma_{-+} + F_{A_1},\\ \dot{A}_2 &= -\frac{\kappa}{2}A_2 + F_{A_2},\end{aligned} \tag{7}$$

where F_{A_1} and F_{A_2} are Langevin noise operators with vanishing mean values. As a matter of fact, these equations for the atomic operators contain higher-order terms involving both field and atomic operators [38–47,49]. This yields a hierarchy of coupled equations. At steady state, we obtain $\langle A_2\rangle = 0$. It is extremely difficult to obtain the stationary state solution to the expectation values of the other operators. We proceed with the case of $\Delta < 0$. The Langevin equations for $A_{1,2}$ are obtainable as

$$\begin{aligned}\dot{A}_1 &= -\frac{\kappa}{2}A_1 + \mathcal{F}_{A_1},\\ \dot{A}_2 &= -\frac{\kappa}{2}A_2 - i\mathcal{G}\sigma_{+-} + \mathcal{F}_{A_2},\end{aligned} \tag{8}$$

where $\mathcal{F}_{A_1}$ and $\mathcal{F}_{A_2}$ are similar Langevin noise operators. Similarly, we arrive at the stationary solution $\langle A_1\rangle = 0$. It is easily seen that the other steady-state solutions are hard to obtain by the same token.

IV. INTERMODE CORRELATION

We first focus on the quantum correlation between the two combination modes. For this purpose, the linear correlation coefficient is defined as

$$C = \frac{\langle\delta N_1\delta N_2\rangle}{\sqrt{\langle(\delta N_1)^2\rangle\,\langle(\delta N_2)^2\rangle}}, \tag{9}$$

where $N_l = A_l^\dagger A_l$ is the photon number operator of the lth combination mode, $(l = 1, 2)$. C has a lower bound 0 and an upper bound 1, which are imposed by the Cauchy-Schwarz inequality. For a two-mode state without intermode correlation, $C = 0$. This is due to the vanishing covariance $\langle\delta N_1\delta N_2\rangle$ in Eq. (9). But for the state $|\psi\rangle_{\rm ss}$ in Eq. (6), we can easily obtain the average photon number in the individual combination mode $\langle N_l\rangle = N$. Correspondingly, the auto and cross correlations are written in a compact form as $\langle\delta N_k\delta N_l\rangle = M^2$,

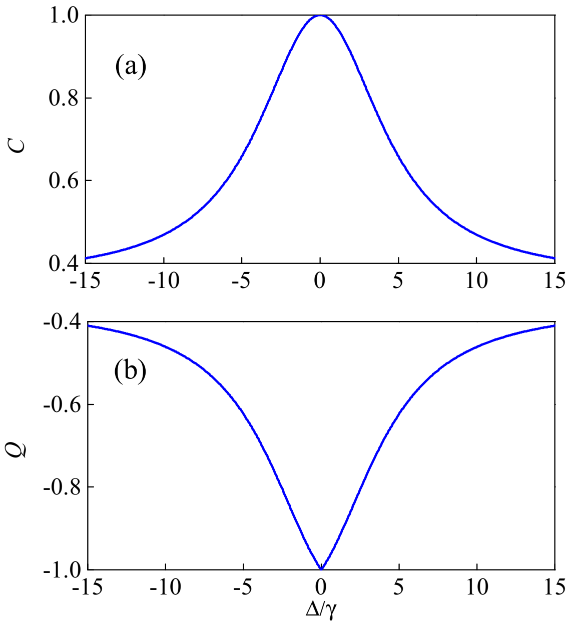

FIG. 2. (a) The intermode correlation C and (b) the Mandel Q parameter as a function of Δ/γ. The parameters are $|\Omega| = 8\gamma$, $|g_1| = |g_2| = 2\gamma$, and $\kappa_1 = \kappa_2 = 3\gamma$.

$(k, l = 1, 2)$. It follows that the pure two-mode squeezed vacuum state always takes the maximum value of 1 and thus exhibits the maximal intermode correlation.

We would like to study the intermode correlation for the current composite system. As shown in Fig. 2(a), the intermode correlation is present over the entire region except $\Delta = 0$. Furthermore, the correlation becomes stronger with the decrease in the magnitude of $|\Delta|$. In the limit of $|\Delta| \to 0$ due to the relaxation the combination modes are led asymptotically to the state $|\psi\rangle_{ss}$. As a result, the maximal intermode correlation emerges asymptotically owing to the mediation of the reservoir. For the sufficiently large values of the detuning Δ, the intermode correlation asymptotically approaches zero (rigorously $C \to 0^+$). This originates from the asymptotic factorization of the numerator in Eq. (9) in such a situation.

V. SUB-POISSONIAN NUMBER DIFFERENCE

We proceed with the quantum fluctuation of the relative number, which is connected to the Mandel Q parameter [24,25,35–37] through the relation

$$Q = \frac{\langle(\delta N_-)^2\rangle}{\langle N_+\rangle} - 1, \tag{10}$$

where $N_\pm = N_1 \pm N_2$, with the denominator representing the sum of the shot-noise figures of the two combination modes [25,35–37]. The Mandel Q parameter is a measure of the photon statistics of a light source, and discloses the departure of the occupation number distribution from Poissonian statistics. The positive values of Q correspond to super-Poissonianity, the zero ones to Poissonianity, and the negative ones to sub-Poissonianity without any classical analog. The Mandel Q parameter has a lower bound -1, corresponding to the perfect squeezing: $\langle(\delta N_-)^2\rangle = 0$. The number difference operator is linked to the state $|\psi\rangle_{ss}$ through the relation: $N_-|\psi\rangle_{ss} = 0$. Therefore, we arrive at $\langle(\delta N_-)^2\rangle = 0$. The pure two-mode squeezed vacuum state has the maximal sub-Poissonian relative number, i.e., $Q = -1$.

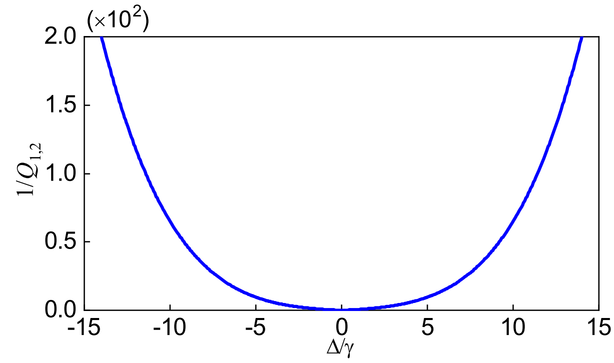

FIG. 3. The inverse of the Mandel parameters $Q_{1,2}$ as a function of Δ/γ. The parameters are the same as those in Fig. 2.

We move to an exploration of how the sub-Poissonian relative number persists for the current system. As shown in Fig. 2(b), the relative number squeezing takes place over the entire region except $\Delta = 0$. Moreover, the sub-Poissonian relative number turns more prominent with the decreasing values of $|\Delta|$. In particular, for $|\Delta| \to 0$, we have $\langle N_l\rangle \to N \to \infty$ and $Q \to -1$, i.e., both of the combination modes are, on the one hand, ultrabright, and on the other hand, possess the ultrastrong number difference squeezing. When the detuning Δ is sufficiently large, the Mandel Q parameter asymptotically approaches zero (rigorously $Q \to 0^-$). The reason is presented as follows. In this extreme case, the autocorrelation (viz., the numerator) in Eq. (10) tends to factorize, and the numerator is ultimately reduced to the sum of the mean photon occupation number per (combination) mode. In other words, we are asymptotically left with the shot-noise limit or standard quantum limit pertaining to the both combination modes. Therefore, the photon statistics is approximate to the Poissonianity, or equivalently, the pair of the combination modes evolves towards the quantum-classical boundary.

In what follows, we would like to explore the photon statistics of these two individual combination modes. The Mandel parameter Q_l for the lth combination mode takes the form as $Q_l = \frac{\langle(\delta N_l)^2\rangle}{\langle N_l\rangle} - 1$, $(l = 1, 2)$. For the two-mode squeezed vacuum state (6), the Mandel parameter of either combination mode is the same and can easily be shown to be $Q_l = \sinh^2 r$. Hence both modes exhibit super-Poissonian photon statistics, and the symmetry between the pair of combination modes is witnessed. We shall discuss how either of their photon-counting statistics depends on the current system parameters. Obviously, either of the combination modes possesses the super-Poissonian statistics over the entire region except $\Delta = 0$, as shown in Fig. 3. With the decrease in the values of $|\Delta|$, the super-Poissonianity is enhanced. In the limit of $|\Delta| \to 0$, Q_l goes to infinity. Likewise at the sufficiently large detunings, Q_l asymptotically goes to zero, i.e., both of the combination modes behave as the optical fields in the coherent states.

VI. VIOLATION OF BELL'S INEQUALITIES

We are now in a position to exploit the Bell test on the two-mode state for a pair of combination modes A_1 and A_2. For this purpose, the Bell inequalities for two modes are mapped into the counterparts for two qubits through the local unconditional transformation. Correspondingly, the single-mode pseudospin (vector) operator $\mathbf{S}$, analogously to the spin angular momentum vector, is introduced and comprised of a triplet of operators $\mathbf{S} = (S_1, S_2, S_3)$ as follows [11]:

$$\begin{aligned} S_1 &= \sum_{n=0}^{\infty} |2n\rangle\langle 2n+1| + |2n+1\rangle\langle 2n|, \\ S_2 &= \frac{1}{i}\sum_{n=0}^{\infty} |2n\rangle\langle 2n+1| - |2n+1\rangle\langle 2n|, \\ S_3 &= \sum_{n=0}^{\infty} |2n\rangle\langle 2n| - |2n+1\rangle\langle 2n+1|, \end{aligned} \tag{11}$$

satisfying the Lie algebra $[S_j, S_k] = 2i\epsilon_{jkl}S_l$ and $S_l^2 = \mathbb{1}$, where ϵ_{jkl} is the Levi-Civita symbol, $j, k, l \in \{1, 2, 3\}$. For the two light fields in the combination modes A_1 and A_2, the Bell operator is defined as

$$\begin{aligned} \mathcal{B} = &(\mathbf{a}\cdot\mathbf{S}^{(1)}) \otimes (\mathbf{b}\cdot\mathbf{S}^{(2)}) + (\mathbf{a}\cdot\mathbf{S}^{(1)}) \otimes (\mathbf{b}'\cdot\mathbf{S}^{(2)}) \\ &+ (\mathbf{a}'\cdot\mathbf{S}^{(1)}) \otimes (\mathbf{b}\cdot\mathbf{S}^{(2)}) - (\mathbf{a}'\cdot\mathbf{S}^{(1)}) \otimes (\mathbf{b}'\cdot\mathbf{S}^{(2)}), \end{aligned} \tag{12}$$

with $\mathbf{a}$, $\mathbf{b}$, $\mathbf{a}'$, and $\mathbf{b}'$ denoting unit vectors in the real three-dimensional space and $\mathbf{S}^{(l)}$ being the pseudospin operator of the lth combination mode, $(l = 1, 2)$. The local hidden variable theory imposes the Bell's inequality

$$|\langle\mathcal{B}\rangle| \leqslant 2, \tag{13}$$

where the angle brackets stand for the averaging over a given two-mode quantum state. The Bell's inequalities in the infinite-dimensional Hilbert space are realized through the joint measurement on dichotomic observable $\mathbf{S}$, in an analogy to the case for the spin formalism.

We proceed to uncover the nonlocality of the light field in the combination modes, and thus invoke the Horodecki nonlocality criterion [7]. The nonlocality is guaranteed if the following inequality is satisfied:

$$B_{\max} = 2\sqrt{u_1 + u_2} > 2, \tag{14}$$

where u_1 and u_2 are two largest eigenvalues of the matrix $\mathbf{U} = \mathbf{V}^T\mathbf{V}$, with the superscript "$T$" representing the transposition and the elements of matrix $\mathbf{V}$ taking the form $V_{kl} = \langle S_k^{(1)} \otimes S_l^{(2)}\rangle$, $(k, l = 1, 2)$. Once the inequality (14) holds, the two-mode quantum state in question displays quantum nonlocality for some vectors $\mathbf{a}$, $\mathbf{b}$, $\mathbf{a}'$, and $\mathbf{b}'$. The maximal Bell violation corresponds to the upper bound $2\sqrt{2}$, which is predicted by quantum mechanics [4]. It is easy to obtain $B_{\max} = 2\sqrt{1+\tanh^2(2r)}$ with respect to the state $|\psi\rangle_{ss}$ in Eq. (6). This is shown by the black dash-dotted line in Fig. 4. It follows that the pure two-mode squeezed vacuum state always violates the Bell's inequalities and hence exhibits nonlocal feature. In the limit of $r \to \infty$, such state approaches the original EPR state. As a consequence, $B_{\max}$ is convergent to the maximum value $2\sqrt{2}$.

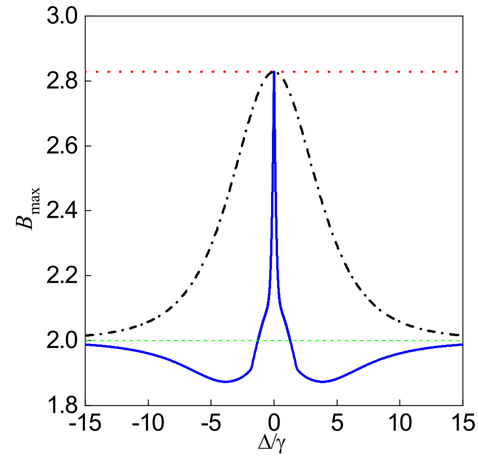

FIG. 4. $B_{\max}$ as a function of Δ/γ. The parameters are the same as those in Fig. 2. The red dotted line stands for the limit set by quantum mechanics, the green dashed line for the limit set by the local hidden variable theory, and the black dash-dotted line for the idealized two-mode squeezed vacuum state (6).

We turn to studying the question as to what extent the nonlocal correlations of the two combination modes should hold when going towards "classical" systems. For the negligibly small detuning, the two-mode state under consideration is close to a pure one. With the increase in the detuning, the combination modes evolve into the mixed states. As depicted in Fig. 4, $B_{\max}$ is larger than 2 in the region $-1.286 \lesssim \Delta/\gamma \lesssim 1.286$ excluding $\Delta = 0$. This discloses the formation of quantum nonlocal states of the two combination modes. In particular, for $|\Delta| \to 0$, $B_{\max}$ converges to the maximum value of $2\sqrt{2}$. The combination modes are eventually pulled by the dissipation into the EPR state which maximally violates the Bell's inequality (13). Beyond the aforementioned parameter regime, one cannot achieve the violation of the Bell's inequalities.

We are now in a position to review the quantum correlations which attract wide interest not only due to their fundamental importance in quantum mechanics, but owing to their promising applications in high-efficiency quantum computation and quantum information tasks. There exists a hierarchy of distinct types of quantum correlations, including quantum entanglement, EPR steering (also called quantum steering), and Bell nonlocality. The EPR steering serves as a bridge between the entanglement and the Bell nonlocality in quantum mechanics, and is viewed as the subtle intermediate quantum correlation in between. Quantum entanglement, quantum steering, and Bell nonlocality all originate from the famous EPR Paradox or "spooky action at a distance" [1], and have no classical counterparts. Not every entangled state is steerable and not all steerable states lead to the violation of Bell's inequality [50]. In other words, all steerable states are entangled, and Bell nonlocality exhibits steering, but not vice versa [12,51–55]. In the language of sets, the steerable states are a strict subset of the entangled states, and a strict superset of the nonlocal Bell states [52]. With reference to Fig. 4, the Bell violation makes it impossible to interpret the nonlocal correlation between the outcomes of measurement on the composite system consisting of the two orthogonal combination modes by use of the local hidden variable theory. Furthermore, the Bell nonlocality implies the two-way EPR steering of the combination modes, and the EPR steering signifies the entanglement between the combination modes. However the reverse is not true [51].

We proceed to identify the difference between the intermode correlation (9) and the entanglement. The intermode correlation (9), which obeys the Cauchy-Schwarz inequality, possesses a classical analog and always has nonnegative values ranging from zero to unity. In a marked contrast, the quasiprobabilities necessarily exhibit negative values for the entangled states [56]. In the field of quantum optics, the negative probability is often employed as an indicator of nonclassicality with regard to the classical statistics [16–18]. The negative probability approach reveals the contradiction between the classical and quantum predictions on the Bell's theorem [2]. The intriguing correlations are found to be stronger than can be interpreted classically. As a fundamental aspect of quantum mechanics, the violation of the Bell's inequalities occurs [57]. The quantum nonlocality is part of a hierarchical structure, i.e., the entangled states constitute a superset of steerable states which, in turn, form a superset of the quantum states with Bell nonlocality. As a classical correlation, the intermode correlation is a necessary condition to exhibit the Bell nonlocality but not a sufficient one. As a consequence, the intermode correlation exists for a large range of detunings but violation of Bell's inequality only happens for a very narrow range of detunings near zero, as shown in Figs. 2(a) and 4.

Before conclusion, we shall make a remark on the advantages of our scheme as follows.

(i) The desired nonclassical state is generated without use (or preparation) of the initially squeezed or entangled sources. Hence no sophisticated experiments is necessitated. Our model may be easier to implement in the laboratory. The pair of original individual cavity modes is coupled directly to the ordinary vacua instead of one or two squeezed vacua, as described by the cavity damping terms in the master equations in Appendixes A and B. Apparently, this is contrary to the schemes in the literature [38–41], where a single-mode squeezed vacuum is injected into the cavity through the (leaky) output end mirror, and hereby of interest are the effects of the squeezed vacuum on the power spectrum of the scattered radiation and the second-order intensity correlation function of the fluorescent light radiated by the atom into the background modes other than the privileged cavity mode. While the measurement of the fluorescence spectrum unveils the information on the first-order correlation function of the light, the measurement on the second-order correlation function discloses the bunching or antibunching effect of the light field. The two-time intensity correlation function of the fluorescent field can be expressed in light of the atomic correlation function [17]. The well-known photon antibunching effect was found in the atomic resonance fluorescence [58]. This is attributed to the quantum nature of the scattering. The detection of one photon pulls the atom into the ground state, so it is very unlikely that another photon emitted from the atomic excited state will be detected simultaneously (with no time delay). While the photon antibunching and sub-Poissonian photon statistics discloses the quantum nature of light, the photon antibunching has a subtle relation to the sub- or super-Poissonian photon-counting statistics. The photon antibunching characterizes the tendency of the photons from a light field to be more equally spaced than those from a coherent laser field. The light beam(s) with the sub-Poissonian photon statistics has (have) less intensity noise compared to the shot-noise figure(s) associated with the beam(s). On the one hand, the sub-Poissonian statistics need not imply photon antibunching, but can be associated with bunching [24]. On the other hand, the antibunching does not necessarily signify sub-Poissonian statistics [27]. While the fluorescence photons always have a tendency to be further apart more frequently than close together, this is not true for the photons in the cavity modes [59]. In addition, it is worth noting that the preparation of the initially squeezed or entangled sources is required in the scheme for the quantum state transfer between the flying photons and stationary atoms [60–63].

(ii) The decoherence pulls the combination modes into the strongly sub-Poissonian nonlocality of radiation by the dissipation. On one side, the decoherence has a tendency to cause the transition from quantum to classical. The exploration of the nonclassical states paves the way for gaining a deep insight into the quantum-classical boundary. On the other side, the decoherence makes possible the generation of a highly Bell nonlocality in the sub-Poissonian regime as the steady state. It should be noted that either of the combination modes exhibits super-Poissonian statistics while their intensity difference noise is reduced to below the shot-noise limit. The desired nonclassical state cannot be achieved without the dissipation of the combination modes. The four-wave mixing process in combination with the suitable choice of the combination modes gives rise to the two-mode squeezed vacuum reservoir, responsible for the emergence of the nonclassicality. Moreover, the nonclassical state is created deterministically by use of the system parameters, which is distinct from those dependent on the probabilistic measurements [64–66]. In this sense, this is an instance of decoherence-assisted formation of the nonclassical states within the framework of cavity quantum electrodynamics. Our scheme is an important step towards the secure quantum communication protocols with the atom-photon interfaces.

VII. CONCLUSION

It is shown how the bright source of strongly sub-Poissonian nonlocality is achieved at steady state. The central focus is on recombining the two photon modes within the cavity and exploring the resultant correlation in the stable state. The physics behind is the four-wave mixing. It is the four-wave mixing process combined with the suitable choice of the combination modes that contributes to the engineered reservoir in the two-mode squeezed vacuum state, and hence enables the generation of bright light beams with strongly sub-Poissonian nonlocality by the relaxation of the dissipative dynamics.

ACKNOWLEDGMENTS

The author gratefully acknowledges the anonymous referee for helpful comments and constructive suggestions. This work is supported by Doctoral Startup Fund of Huainan Normal University.

APPENDIX A: MASTER EQUATION IN THE BARE-STATE REPRESENTATION

The time evolution of the current composite system can be described by the reduced density operator ρ, which obeys the master equation in an appropriate rotating frame and in the dipole approximation as

$$\dot{\rho} = -\frac{i}{\hbar}[H_1 + H_2, \rho] + \mathcal{L}_{\rm sp}\rho + \mathcal{L}_{\rm cav}\rho, \tag{A1}$$

where the Hamiltonians take the form

$$\begin{aligned} H_1 &= \hbar\Delta\sigma_{22} + \frac{\hbar}{2}(\Omega\sigma_{21} + \Omega^*\sigma_{12}), \\ H_2 &= \hbar(g_1 a_1\sigma_{21}\, e^{-i\delta_1 t} + g_2 a_2\sigma_{21}\, e^{-i\delta_2 t}) + \text{ H.c.} \end{aligned} \tag{A2}$$

Here H_1 stands for the free Hamiltonian for the atom and the coupling of the atom to the external field, and H_2 describes the interaction of the atom with the cavity fields. a_l and $a_l^\dagger$ are the annihilation and creation operators. $\sigma_{kl} = |k\rangle\langle l|$ are the usual atomic operators $(k, l = 1, 2)$. $\Delta = \omega_{21} - \omega_L$ is the detuning of the atomic resonance transition frequency ω_{21} from the driving field frequency $\omega_{\rm L}$. $\delta_l = \nu_l - \omega_L$ are the detunings of the cavity-mode frequencies ν_l from the driving field frequency ω_L. $\mathcal{L}_{\rm sp}\rho$ and $\mathcal{L}_{\rm cav}\rho$ represent the damping of the atom by spontaneous emission with the rate γ and that of the cavity fields a_l by cavity decay with the rates κ_l, and take the form

$$\begin{aligned} \mathcal{L}_{\rm sp}\rho &= \gamma\mathcal{D}[\sigma_{12}]\rho, \\ \mathcal{L}_{\rm cav}\rho &= \sum_{l=1,2}\kappa_l\mathcal{D}[a_l]\rho, \end{aligned} \tag{A3}$$

where the superoperator $\mathcal{D}[O]\rho$ is defined as $\mathcal{D}[O]\rho = O\rho O^\dagger - \frac{1}{2}(O^\dagger O\rho + \rho O^\dagger O)$.

APPENDIX B: MASTER EQUATION IN THE DRESSED-STATE PICTURE

We would like to eliminate the exponential factors of the Hamiltonian H_2 in Eq. (A2) through a unitary transformation. For this purpose, we make the substitution $|1\rangle \to |1\rangle\, e^{i\phi_0}$, $a_1 \to a_1\, e^{i(\phi_0-\phi_1)}$, and $a_2 \to -a_2\, e^{i(\phi_0-\phi_2)}$, where $\phi_0 = \arg(\Omega)$, $\phi_l = \arg(g_l)$, $(l = 1, 2)$. The dressed states are obtained, see Eq. (3) in the main text. The eigenenergies are $\mathcal{E}_\pm = \hbar\lambda_\pm$, with $\lambda_\pm = \frac{1}{2}(\Delta \pm \Omega_R)$ and $\Omega_R = \sqrt{\Delta^2 + |\Omega|^2}$. Thus the Hamiltonian H_1 in Eq. (A2) is transformed to the diagonal form as $H_1 \to \tilde{H}_1 = \hbar\lambda_+\sigma_{++} + \hbar\lambda_-\sigma_{--}$.

Here we are confined to the case of $\delta_1 = -\delta_2 = \Omega_{\rm R}$. We then perform the unitary transformation with the unitary operator $\mathcal{U} = \exp(-\frac{i}{\hbar}\tilde{H}_1 t)$, and ignore the rapidly oscillating terms. The master equation is derived in the dressed-state picture as

$$\dot{\varrho} = -\frac{i}{\hbar}[\mathcal{H}_{\rm r} + \mathcal{H}_{\rm b}, \varrho] + \mathcal{L}_{\rm at}\varrho + \mathcal{L}_{\rm cav}\varrho, \tag{B1}$$

where $\varrho = \mathcal{U}\rho\mathcal{U}^\dagger$, $\mathcal{H}_r$, and $\mathcal{H}_b$ are written in the form

$$\begin{aligned} \mathcal{H}_{\rm r} &= \hbar\tilde{g}_1 a_1\sigma_{+-} + \text{ H.c.}, \\ \mathcal{H}_{\rm b} &= \hbar\tilde{g}_2 a_2^\dagger\sigma_{+-} + \text{H.c.}, \end{aligned} \tag{B2}$$

with $\tilde{g}_1 = |g_1|\cos^2\theta$ and $\tilde{g}_2 = |g_2|\sin^2\theta$. The damping terms in the master equation (A1) are cast into the form

$$\begin{aligned} \mathcal{L}_{\rm at}\varrho &= \sum_{j=1}^{3}\Gamma_j\mathcal{D}[O_j]\varrho, \\ \mathcal{L}_{\rm cav}\varrho &= \sum_{l=1,2}\kappa_l\mathcal{D}[a_l]\varrho, \end{aligned} \tag{B3}$$

where O_j and Γ_j are explicitly shown in the main text.

APPENDIX C: CONSTRUCTION OF THE SQUEEZE OPERATOR

This section is dedicated mainly to constructing the two-mode squeeze operator in attempt to gain a deep insight into the dynamics and physical mechanism. Without loss of generality, we are concerned with the consumption of $|g_1| = |g_2| = \mathfrak{g}$, and arrive at

$$\mathcal{H}_{\rm r} + \mathcal{H}_{\rm b} = \hbar\mathfrak{g}(a_1\cos^2\theta + a_2^\dagger\sin^2\theta)\sigma_{+-} + \text{ H.c.} \tag{C1}$$

In what follows, we shall discuss three cases in terms of the dressed states (3) in the main text.

(i) $\Delta > 0$, i.e., $\theta = \theta_1 \in (0, \pi/4)$.

We first define $\tanh r_1 = \tan^2\theta_1 < 1$ and then obtain

$$\mathcal{H}_{\rm r} + \mathcal{H}_{\rm b} = \hbar\mathfrak{g}\sqrt{\cos(2\beta_1)}A_1\sigma_{+-} + \text{H.c.}, \tag{C2}$$

where the combination mode A_1 takes the form

$$A_1 = a_1\cosh r_1 + a_2^\dagger\sinh r_1, \tag{C3}$$

with $\beta_1 = \frac{1}{2}\arctan(\frac{|\Omega|}{\Delta})$.

(ii) $\Delta < 0$, i.e., $\theta = \theta_2 \in (\pi/4, \pi/2)$.

We define $\tanh r_2 = \cot^2\theta_2 < 1$ and find

$$\begin{aligned} \mathcal{H}_{\rm r} + \mathcal{H}_{\rm b} &= \hbar\mathfrak{g}\sqrt{|\cos(2\theta_2)|}\,A_2^\dagger\sigma_{+-} + \text{H.c.} \\ &= \hbar\mathfrak{g}\sqrt{\cos(2\beta_2)}\,A_2^\dagger\sigma_{+-} + \text{H.c.}, \end{aligned} \tag{C4}$$

where the combination mode A_2 is given by

$$A_2 = a_2\cosh r_2 + a_1^\dagger\sinh r_2, \tag{C5}$$

with $\beta_2 = \frac{1}{2}\arctan(\frac{|\Omega|}{|\Delta|})$.

It is easy to see

$$\tanh r_1 = \tanh r_2 = \tan^2\theta_1 = \cot^2\theta_2, \tag{C6}$$

for a fixed value of $|\Delta|$ with opposite sign of the detuning Δ. Here we invoked the trigonometric identities $\text{arccot}(-x) = \pi - \text{arccot}(x)$ and $\arctan(x) + \text{arccot}(x) = \pi/2$, $(x \in \mathbb{R})$. Finally, the two combination modes of concern are written as

$$\begin{aligned} A_1 &= a_1\cosh r + a_2^\dagger\sinh r, \\ A_2 &= a_2\cosh r + a_1^\dagger\sinh r, \end{aligned} \tag{C7}$$

where $\tanh r = \tan^2\beta$, with $\beta = \frac{1}{2}\arctan\frac{|\Omega|}{|\Delta|}$. The pair of modes A_l is connected to the original individual operators a_l through the relation $A_l = \mathcal{S}a_l\mathcal{S}^\dagger$ $(l = 1, 2)$, where the squeeze operator of concern is expressed in the form

$$\mathcal{S} = \exp(ra_1a_2 - ra_1^\dagger a_2^\dagger). \tag{C8}$$

It is apparent to obtain

$$\mathcal{H}_{\rm r}+\mathcal{H}_{\rm b}=\begin{cases}\hbar\mathcal{G}A_1\sigma_{+-}+\text{H.c.}, & \text{if } \Delta>0,\\ \hbar\mathcal{G}A_2^{\dagger}\sigma_{+-}+\text{H.c.}, & \text{if } \Delta<0,\end{cases} \tag{C9}$$

which is, in essence, equivalent to Eq. (2) in the main text, together with $\mathcal{G}=\mathfrak{g}\sqrt{\cos(2\beta)}$. Furthermore, the second equation in Eq. (B3) can be reexpressed in terms of Eq. (C7) as the same form as that in Eq. (5).

(iii) $\Delta=0$, i.e., $\theta=\pi/4$.

In this case we cannot achieve the two-mode squeeze operator or squeezing transformation.

[1] A. Einstein, B. Podolsky, and N. Rosen, Phys. Rev. **47**, 777 (1935).
[2] J. S. Bell, Physics (Long Island City, N.Y.) **1**, 195 (1964).
[3] J. F. Clauser, M. A. Horne, A. Shimony, and R. A. Holt, Phys. Rev. Lett. **23**, 880 (1969).
[4] B. S. Cirelson, Lett. Math. Phys. **4**, 93 (1980).
[5] L. J. Landau, Phys. Lett. A **120**, 54 (1987).
[6] S. L. Braunstein, A. Mann, and M. Revzen, Phys. Rev. Lett. **68**, 3259 (1992).
[7] R. Horodecki, P. Horodecki, and M. Horodecki, Phys. Lett. A **200**, 340 (1995).
[8] H. Halvorson, Lett. Math. Phys. **53**, 321 (2000).
[9] K. Banaszek and K. Wódkiewicz, Phys. Rev. A **58**, 4345 (1998); Phys. Rev. Lett. **82**, 2009 (1999).
[10] H. Jeong, W. Son, M. S. Kim, D. Ahn, and Č. Brukner, Phys. Rev. A **67**, 012106 (2003).
[11] Z. B. Chen, J. W. Pan, G. Hou, and Y. D. Zhang, Phys. Rev. Lett. **88**, 040406 (2002).
[12] H. M. Wiseman, S. J. Jones, and A. C. Doherty, Phys. Rev. Lett. **98**, 140402 (2007).
[13] N. Brunner, D. Cavalcanti, S. Pironio, V. Scarani, and S. Wehner, Rev. Mod. Phys. **86**, 419 (2014).
[14] A. K. Ekert, Phys. Rev. Lett. **67**, 661 (1991).
[15] N. Gisin and B. Huttner, Phys. Lett. A **228**, 13 (1997).
[16] M. O. Scully and M. S. Zubairy, *Quantum Optics* (Cambridge University Press, Cambridge, England, 1997).
[17] D. F. Walls and G. J. Milburn, *Quantum Optics*, 2nd ed. (Springer-Verlag, Berlin, 2008).
[18] M. Orszag, *Quantum Optics*, 3rd ed. (Springer-Verlag, Switzerland, 2006).
[19] E. M. Purcell, Phys. Rev. **69**, 681 (1946).
[20] D. Kleppner, Phys. Rev. Lett. **47**, 233 (1981).
[21] C. H. Keitel, P. L. Knight, L. M. Narducci, and M. O. Scully, Opt. Commun. **118**, 143 (1995).
[22] A. S. Parkins, E. Solano, and J. I. Cirac, Phys. Rev. Lett. **96**, 053602 (2006).
[23] S. Pielawa, G. Morigi, D. Vitali, and L. Davidovich, Phys. Rev. Lett. **98**, 240401 (2007).
[24] L. Mandel and E. Wolf, Rev. Mod. Phys. **37**, 231 (1965); L. Mandel, Opt. Lett. **4**, 205 (1979); X. T. Zou and L. Mandel, Phys. Rev. A **41**, 475 (1990); L. Mandel and E. Wolf, *Optical Coherence and Quantum Optics* (Cambridge University Press, Cambridge, England, 1995).
[25] J.-C. Jaskula, M. Bonneau, G. B. Partridge, V. Krachmalnicoff, P. Deuar, K. V. Kheruntsyan, A. Aspect, D. Boiron, and C. I. Westbrook, Phys. Rev. Lett. **105**, 190402 (2010).
[26] R. E. Slusher, L. W. Hollberg, B. Yurke, J. C. Mertz, and J. F. Valley, Phys. Rev. Lett. **55**, 2409 (1985); **56**, 788 (1986).
[27] L. Davidovich, Rev. Mod. Phys. **68**, 127 (1996).
[28] C. Cohen-Tannoudji, J. Dupont-Roc, and G. Grynbery, *Atom-Photon Interactions* (Wiley, New York, 1992).
[29] G. S. Agarwal and R. W. Boyd, Phys. Rev. A **38**, 4019 (1988).
[30] V. Boyer, A. M. Marino, R. C. Pooser, and P. D. Lett, Science **321**, 544 (2008).
[31] I. Allayarov, M. A. Schmidt, and T. Weiss, Phys. Rev. A **101**, 043806 (2020).
[32] J. W. You, Z. H. Lan, and N. C. Panoiu, Sci. Adv. **6**, eaaz3910 (2020).
[33] R. W. Boyd, *Nonlinear Optics*, 4th ed. (Academic, San Diego, CA, 2020).
[34] A. M. Marino, V. Boyer, R. C. Pooser, P. D. Lett, K. Lemons, and K. M. Jones, Phys. Rev. Lett. **101**, 093602 (2008).
[35] Z. Z. Qin, L. M. Cao, H. L. Wang, A. M. Marino, W. P. Zhang, and J. T. Jing, Phys. Rev. Lett. **113**, 023602 (2014).
[36] Z. Q. Yang, P. Saurabh, F. Schlawin, S. Mukamel, and K. E. Dorfman, Appl. Phys. Lett. **116**, 244001 (2020).
[37] K. Dorfman, S. S. Liu, Y. B. Lou, T. X. Wei, J. T. Jing, F. Schlawin, and S. Mukamel, Proc. Natl. Acad. Sci. USA **118**, e2105601118 (2021).
[38] J. I. Cirac and L. L. Sanchez-Soto, Phys. Rev. A **44**, 1948 (1991); J. I. Cirac, *ibid.* **46**, 4354 (1992).
[39] P. R. Rice and L. M. Pedrotti, J. Opt. Soc. Am. B **9**, 2008 (1992); P. R. Rice and C. A. Baird, Phys. Rev. A **53**, 3633 (1996).
[40] W. S. Smyth and S. Swain, Phys. Rev. A **53**, 2846 (1996).
[41] D. Erenso and R. Vyas, Phys. Rev. A **65**, 063808 (2002).
[42] X. X. Li and X. M. Hu, Phys. Rev. A **80**, 023815 (2009).
[43] J. Y. Li and X. M. Hu, Phys. Rev. A **80**, 053829 (2009).
[44] X. Zhang and X. M. Hu, Phys. Rev. A **81**, 013811 (2010).
[45] F. Wang, X. M. Hu, W. X. Shi, and Y. Z. Zhu, Phys. Rev. A **81**, 033836 (2010).
[46] Q. Xu and X. M. Hu, Phys. Rev. A **86**, 032337 (2012).
[47] X. Liang, X. M. Hu, and C. He, Phys. Rev. A **85**, 032329 (2012).
[48] M. Sargent III, M. O. Scully, and W. E. Lamb, Jr., *Laser Physics* (Addison Wesley, Reading, MA, 1974).
[49] Q. Xu and X. M. Hu, Chin. Phys. Lett. **28**, 074217 (2011).
[50] W. Y. Sun, D. Wang, J. D. Shi, and L. Ye, Sci. Rep. **7**, 39651 (2017).
[51] M. T. Quintino, T. Vértesi, D. Cavalcanti, R. Augusiak, M. Demianowicz, A. Acín, and N. Brunner, Phys. Rev. A **92**, 032107 (2015).
[52] S. J. Jones, H. M. Wiseman, and A. C. Doherty, Phys. Rev. A **76**, 052116 (2007).
[53] K. Sun, X. J. Ye, Y. Xiao, X. Y. Xu, Y. C. Wu, J. S. Xu, J. L. Chen, C. F. Li, and G. C. Guo, npj Quantum Inf. **4**, 12 (2018).
[54] Y. Y. Zhao, H. Y. Ku, S. L. Chen, H. B. Chen, F. Nori, G. Y. Xiang, C. F. Li, G. C. Guo, and Y. N. Chen, npj Quantum Inf. **6**, 77 (2020).

[55] Y. Z. Zhen, X. Y. Xu, L. Li, N. L. Liu, and K. Chen, Entropy **21**, 422 (2019).
[56] J. Sperling and W. Vogel, Phys. Rev. A **79**, 042337 (2009).
[57] S. Storz *et al.*, Nature (London) **617**, 265 (2023).
[58] H. J. Kimble, M. Dagenais, and L. Mandel, Phys. Rev. Lett. **39**, 691 (1977); Phys. Rev. A **18**, 201 (1978).
[59] Q. Xu and K. Mølmer, J. Phys. B: At. Mol. Opt. Phys. **50**, 035502 (2017).
[60] K. S. Choi, H. Deng, J. Laurat, and H. J. Kimble, Nature (London) **452**, 67 (2008).
[61] B. Julsgaard, A. Kozhekin, and E. S. Polzik, Nature (London) **413**, 400 (2001).
[62] T. Wilk, S. C. Webster, A. Kuhn, and G. Rempe, Science **317**, 488 (2007).
[63] D. N. Matsukevich, T. Chanelière, S. D. Jenkins, S.-Y. Lan, T. A. B. Kennedy, and A. Kuzmich, Phys. Rev. Lett. **96**, 030405 (2006).
[64] B. B. Blinov, D. L. Moehring, L. M. Duan, and C. Monroe, Nature (London) **428**, 153 (2004).
[65] J. Volz, M. Weber, D. Schlenk, W. Rosenfeld, J. Vrana, K. Saucke, C. Kurtsiefer, and H. Weinfurter, Phys. Rev. Lett. **96**, 030404 (2006).
[66] C. W. Chou, H. de Riedmatten, D. Felinto, S. V. Polyakov, S. J. van Enk, and H. J. Kimble, Nature (London) **438**, 828 (2005).